

Numerical simulation of the fire emergency evacuation for a metro platform accident

Jiabin Xie, Kecheng Chen, Trevor Hocksun Kwan and Qinghe Yao 

Abstract

A coupled analysis of agent behavior and Computational Fluid Dynamics (CFD) model is applied to investigate the fire evacuation effectiveness in a popular metro station in Guangzhou, China. Due to the high density and complexity of traffic, the concept of Required Safe Escape Time and Available Safe Escape Time (RSET/ASET), which is more flexible and adaptable than the “6 minutes” principle, is applied in the safety assessment of fire evacuation. To pursue a stable simulation of the coupled model, the standard Critical Radiant Flux is used to deter the tenability criteria for exposure to fire and heat. Various related factors, including the fire location, the Heat Release Rate (HRR) of fire, the crowd density, and the operation mode of escalators, are analyzed through a series of simulations. Results indicate that the interaction between fire and humans should not be neglected in the evacuation simulation. Both the fire location and the crowd density have a significant effect on the evacuation, while the HRR of fire has a minor impact. When the accident happens at the entrance of an escalator, RSET is 58.3% longer than that when the accident occurs in the middle of the platform. RSET grows with the increase of the crowd density linearly. Besides, the evacuation efficiency could be partly improved by changing escalators that usually operate in the descending mode into ascending mode.

Keywords

Emergency evacuation, coupled analysis, agent-based evacuation model, metro platform fire

1. Introduction

Fire evacuation modeling is a field of science which relates to the simulation of human behavior during fire emergencies.¹ Various pedestrian dynamics models—which can be divided into two types, the macroscopic model and the microscopic model—have been developed in past research. A typical macroscopic model is the fluid dynamics model²; however, it takes little consideration of the impact of human factors. Microscopic models, such as the cellular automata model,³ the social force model,⁴ and the lattice gas model,⁵ perform relatively better in reflecting the mutual influence of individuals.

There has been much research on fire evacuation in the metro station. For some the main focus is on the analysis of the fire environment, such as the temperature distribution and the smoke spread,^{6–8} which is a significant reference when determining the fire evacuation scheme. The ventilation system is one of the principal factors affecting the smoke flow and the thermal environment in the metro station. The optimal ventilation mode varies with the type of metro station as well as its inner layout.^{9–12} Recently,

the platform screen door (PSD) is increasingly installed, and provides many benefits to passengers’ safety. In the work of Zhou et al.,¹³ PSD plays a remarkable role in restricting the diffusion of smoke. Roh et al.^{14,15} concluded that passengers on a platform with PSD and ventilation system have much more available time; other researchers place particular emphasis on the simulation of the fire evacuation process.^{16,17} Downward evacuation, proposed by Tsukahara et al.,¹⁸ which is in the opposite direction to the smoke flow, can be more effective than upward evacuation for a large-scale subway fire. Wan et al.¹⁹ proposed a modified combined social force model and found that the wind speed and the toxic gas sources have a significant effect on casualties. The interaction

School of Aeronautics and Astronautics, Sun Yat-Sen University, Guangzhou, China

Corresponding author:

Qinghe Yao, School of Aeronautics and Astronautics, Sun Yat-Sen University, Guangzhou, Guangdong 510275, China.
Email: yaoqhe@mail.sysu.edu.cn

between fire and human should not be neglected. Frantzich and Nilsson²⁰ found that the walking speed of humans decreases with increasing smoke concentration. Yang et al.²¹ found that the fire increases the air temperature and the smoke density, leading to a decrease in pedestrians' visibility and walking speed. The fire location also influences the evacuation.²² Nevertheless, to the best of the authors' knowledge, just a few studies have coupled the fire development and the evacuation process together.

Service facilities such as automatic ticket gates, stairways, and escalators are significant factors affecting fire evacuation in the metro station. The automatic ticket gate has been recognized as an evacuation bottleneck.^{23,24} Characteristics of a crowd flow passing through ticket gates were identified in detail,²⁵⁻²⁷ based on which some optimization design methods were proposed.^{28,29} Escalators are becoming increasingly common in newly built metro stations in China. Because they have a higher passing capacity than the stairway, escalators have been considered to be utilized for emergency evacuation.^{30,31} The operation mode of escalators is an issue worthy of further study.^{16,32}

Currently, the fire safety design of metro station mainly follows the requirements of the design code of metro (GB 50157 – 2013), that is the prescriptive-based design. Fire safety designers have to ensure that all passengers in the train and on the platform can timely evacuate to safe regions in 6 minutes; this is called the “6 minutes” principle.³³ By contrast, the widely accepted concept in performance-based design, Required Safe Escape Time (RSET) and Available Safe Escape Time (ASET), is more flexible and adaptable than the “6 minutes” principle when being applied to a complicated fire scenario. ASET is the amount of time that elapses between fire ignition and the development of untenable conditions, whereas RSET is the amount of time required for occupants to evacuate a building or space and reach a safe place. RSET/ASET comparison enables the influence of each parameter on the performance of the fire safety system to be evaluated.³⁴ However, as research on the design of performance-based fire protection began late in China, RSET/ASET is rarely used for the safety assessment of fire evacuation in a metro station in China. Concerning the calculation of ASET, most researchers treat the exposure of skin to radiant heat in a relatively simplified way.³⁵ The standard of Critical Radiant Flux (CRF), 2.5 kW/m², which is often hard to measure in the designing process, and most scholars apply it indirectly with the corresponding smoke layer temperature (about 180°C).^{36,37}

Higher Education Mega Center North, a popular metro station in the higher education mega center of Guangzhou, sitting in an isolated island, which is a typical side platform station, is taken as the example to investigate in this work as it is the main entrance for students to enter the island. The station serves more than 10 colleges and

universities; without clear and practical emergency plans, the lives of people in such a crowded station would be under threat. The fire emergency evacuation simulator, a coupled program of an agent-based evacuation model and a Computational Fluid Dynamics (CFD) model, is applied to study the fire evacuation considering the interaction between fire and humans. The influences of the location and the Heat Release Rate (HRR) of fire and the crowd density on the fire evacuation are studied. In addition, how to operate the escalator to improve the evacuation efficiency in the case of fire is analyzed. Furthermore, RSET/ASET is applied for the safety assessment of fire evacuation. As the smoke layer is unstable in the simulation, thus substituting CRF with the corresponding smoke layer temperature is undesirable, it is applied directly to deter the tenability criteria for exposure to fire and heat.

The rest of this paper is as follows. The CFD fire model and agent-based evacuation model in the fire emergency evacuation simulator concerning the implementation of fire evacuation coupled simulation are briefly illustrated in Section 2. In Section 3, the concept of RSET /ASET for the safety assessment of fire evacuation is introduced. The settings of tenability criteria used for the calculation of ASET are emphasized. In Section 4, the investigated metro station is introduced, and principal characteristics of fire and passengers are determined. A series of fire scenarios are developed for the subsequent simulations, considering different factors including the fire location, the HRR of fire, the crowd density, and the operation mode of escalators. The simulation results are presented in Section 5. This paper ends with the conclusion and future work in Section 6.

2. Implementation of fire evacuation coupled simulation

The fire emergency evacuation simulator (FDS + Evac) is a coupled program of an agent-based evacuation calculation model and a CFD model of fire-driven fluid flow. The interactions between fire and human behavior are considered in the simulation: fire influences evacuation conditions by affecting the movement and decision making of the humans and blocking major exit routes in extreme cases; on the other hand, humans influence the fire by opening doors or actuating various fire protection devices. As illustrated in Figure 1, all fire-related quantities, such as smoke concentration, toxic gases concentration, and gases temperature, are first calculated by the CFD fire model and then applied to the evacuation calculation. The effect of smoke on the movement speeds of agents and the toxic influence of the smoke are implemented in the simulation. Furthermore, the exit selection algorithm of the agents uses smoke concentration to calculate the visibility of the exit doors and to categorize the entries into different

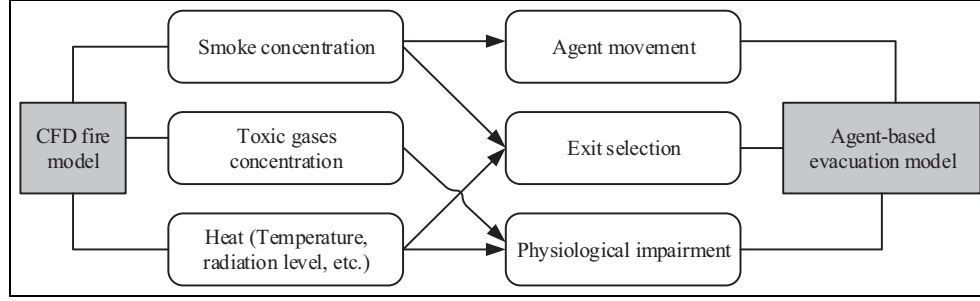


Figure 1. Implementation of fire evacuation coupled simulation.

preference levels. The cores of the CFD fire model and the agent-based evacuation model are briefly illustrated as follows.

2.1. CFD fire model

2.1.1. Hydrodynamic model. The fire emergency evacuation simulator solves a form of the Navier–Stokes equations appropriate for low-speed, thermally driven flow numerically with an emphasis on smoke and heat transport from fires. The core algorithm is an explicit predictor-corrector scheme, second-order accurate in space and time.³⁸ By default, turbulence is treated using Large Eddy Simulation.

2.1.2. Numerical grid. The governing equations are approximated on a collection of uniformly spaced three-dimensional staggered grids. The whole computational domain can be broken into multiple meshes and then processed in parallel using Message Passing Interface (MPI). OpenMP is also available to speed up the processing of a given mesh. Rectangular obstructions are simply defined on the underlying grid and treated by a direct-forcing immersed boundary method.

2.1.3. Mass and species transport. The number of fuels is limited to one, and the number of reactions is limited to one or two to make the simulations tractable. At least six gas species (Fuel, O₂, CO₂, H₂O, CO, N₂) and soot particulate need to be tracked in the simulation. To realize species mass fractions, the strategy is to solve a transport equation for the mass density of each species and then to obtain the mixture mass density by summation of the species' densities.

2.1.4. Momentum transport. Noting the vector identity $(\mathbf{u} \cdot \nabla)\mathbf{u} = \frac{\nabla|\mathbf{u}|^2}{2} - \mathbf{u} \times \mathbf{w}$, and defining the stagnation energy per unit mass, $H \equiv \frac{|\mathbf{u}|^2}{2} + \frac{p}{\rho}$, the momentum equation can be written as:

$$\begin{aligned} \frac{\partial \mathbf{u}}{\partial t} - \mathbf{u} \times \mathbf{w} + \nabla H - \tilde{p} \nabla \left(\frac{1}{\rho} \right) \\ = \frac{1}{\rho} [(\rho - \rho_0)\mathbf{g} + \mathbf{f}_b + \nabla \cdot \boldsymbol{\tau}], \end{aligned} \quad (1)$$

where \mathbf{f}_b is the drag force exerted by the subgrid-scale particles and droplets, \tilde{p} is the pressure perturbation, \mathbf{g} is the gravity vector, normally $(0,0,-g)$, and $\boldsymbol{\tau}$ is the viscous stress which is closed via gradient diffusion with the turbulent viscosity obtained from the Deardorff eddy viscosity model.^{39,40} Equation (4) is convenient to be written in the form of:

$$\frac{\partial \mathbf{u}}{\partial t} + \mathbf{F} + \nabla H = 0. \quad (2)$$

So that a Poisson equation for the pressure can be derived by taking its divergence as follows:

$$\nabla^2 H = - \left[\frac{\partial}{\partial t} (\nabla \cdot \mathbf{u}) + \nabla \cdot \mathbf{F} \right]. \quad (3)$$

It is solved by a kind of fast FFT-based direct solver optimized for uniform grids.⁴¹

2.1.5. Combustion and radiation. Combustion and radiation are introduced into the governing equations via the source terms, \dot{q}''' and \dot{q}_r''' in the energy transport equation. The combustion model is based on the mixing-limited, infinitely fast reaction of lumped species (a species representing a group of species). These lumped species are air, fuel, and products. For an infinitely fast reaction, reactant species in a given grid cell are converted to product species at a rate determined by a characteristic mixing time, τ_{mix} . The HRR per unit volume is defined by summing the lumped species mass production rates times their respective heats of formation.

In the model, radiative heat transfer is included via the solution of the radiation transport equation for a gray gas, and in some limited cases using a wideband model. The

governing equations are solved using a technique similar to finite volume methods for convective transport. The model also includes the absorption and scattering of thermal radiation from water droplets.

2.2. Agent-based evacuation model

2.2.1. Agent movement model. The agent movement model is the basis of the evacuation model. The Social Force Model by Helbing and Molnár⁴ is used as the starting point of the agent movement algorithm of the fire emergency evacuation simulator. Each agent follows its equation of motion as follows:

$$m_i \frac{d^2 \mathbf{x}_i(t)}{dt^2} = \mathbf{f}_i(t) + \boldsymbol{\xi}_i(t), \quad (4)$$

where $\mathbf{x}_i(t)$ is the position of agent i at time t , $\mathbf{f}_i(t)$ is the force exerted on agent i by the surroundings, m_i is the mass, and the last term, $\boldsymbol{\xi}_i(t)$, is a small random fluctuation force.

The force on the agent i has many components:

$$\begin{aligned} \mathbf{f}_i = & \frac{m_i}{\tau_i} (\mathbf{v}_i^0 - \mathbf{v}_i) + \sum_{j \neq i} (\mathbf{f}_{ij}^{soc} + \mathbf{f}_{ij}^c + \mathbf{f}_{ij}^{att}) \\ & + \sum_w (\mathbf{f}_{iw}^{soc} + \mathbf{f}_{iw}^c) + \sum_k \mathbf{f}_{ik}^{att}. \end{aligned} \quad (5)$$

The first term on the right-hand side describes the motive force on the evacuating agent. \mathbf{v}_i^0 is the expected walking velocity of each agent. The relaxation time parameter τ_i sets the strength of the motive force. The first sum describes interactions between agent i and j . The sum over w describes interactions between agent i and the wall. It is worth noting that the term in the last sum, \mathbf{f}_{ik}^{att} , may be used for other agent–environment interactions, such as the fire–agent repulsion. However, this kind of interaction has not yet been implemented in the simulator. More detail concerning the calculation of these three kinds of interactions, please refer to Helbing et al. and Korhonen.^{42,43}

Smoke reduces the walking speed of humans because of the reduced visibility as well as irritating and asphyxiant effects. The walking speed of agent i in smoke, $v_i^0(K_s)$, may be expressed by the following formula^{20,43}:

$$v_i^0(K_s) = \max \left\{ v_{i, \min}^0, v_i^0 \left(1 + \frac{\beta}{\alpha} K_s \right) \right\}, \quad (6)$$

where the minimum walking speed of agent i is $v_{i, \min}^0 = 0.1 \cdot v_i^0$ by default, the values of the coefficients α and β are 0.706 m/s and $-0.057 \text{ m}^2/\text{s}$, and K_s is the extinction coefficient that is proportional to the smoke density.

2.2.2. Physiological impairment. Both toxic gases and untenable heat produced by fire can lead to physiological impairment.⁴⁴ For now, only toxic effects of gaseous fire products are considered and treated by using Purser's

Fractional Effective Dose (FED) concept.⁴⁵ The FED value is calculated as:

$$\begin{aligned} \text{FED}_{\text{tot}} = & (\text{FED}_{\text{CO}} + \text{FED}_{\text{CN}} + \text{FED}_{\text{NO}_x} + \text{FLD}_{\text{irr}}) \\ & \times \text{HV}_{\text{CO}_2} + \text{FED}_{\text{O}_2}. \end{aligned} \quad (7)$$

Note that the gas–phase concentrations of O_2 (percent), CO_2 (percent), and CO (ppm) are used by default to calculate the FED index. They are calculated as:

$$\text{FED}_{\text{CO}} = \int_0^t 2.764 \times 10^{-5} (C_{\text{CO}}(t))^{1.036} dt, \quad (8)$$

$$\text{HV}_{\text{CO}_2} = \frac{\exp(0.1903 C_{\text{CO}_2}(t) + 2.0004)}{7.1}, \quad (9)$$

$$\text{FED}_{\text{O}_2} = \int_0^t \frac{dt}{60 \exp[8.13 - 0.54(20.9 - C_{\text{O}_2}(t))]} \quad (10)$$

The effects of some other gases (NO , NO_2 , CN , HCl , HBr , HF , SO_2 , $\text{C}_3\text{H}_4\text{O}$, CH_2O) are also considered if needed. An agent is considered to be incapacitated when the FED value exceeds 1. The incapacitated agent stops immediately and does not experience social forces anymore.

2.2.3. Exit selection. The exit selection algorithm of the fire emergency evacuation simulator is based on a game-theoretic model described and analyzed in detail by Korhonen and Hostikka,⁴⁶ and Ehtamo et al.^{47,48} The agents observe the actions of the others and select the target exit through which the evacuation is estimated to be the fastest. The evacuation time of each agent to each exit is calculated from the distances to the exits and the congestion in front of the exits. The walking time to the exit door is simply approximated by dividing the distance to the door by the unimpeded walking velocity of the agent. The queuing time is calculated by dividing the number of agents closer to the door than the present one by an estimated flow through the door. The estimated flow is given by the door width times the specific flow value specified by the user. The presently chosen door is preferred, and 10% longer time is tolerated by default.

Three other criteria affecting the exit selection are the visibility of the exits, the fire-related disturbing condition, and the familiarity with exits. The visibility of an exit to an agent is determined by the blocking effect of smoke. The user gives a threshold visibility value for a door to be considered as a “smoke-free” door. A door is usable as long as the visibility is larger than half the distance to the door, where local visibility = 3/extinction coefficient. Under the same visibility, it is assumed that the agents prefer more familiar routes than others. The familiarity of each exit for each agent can be determined by the user. It is also possible to give a probability for the familiarity of an exit. The

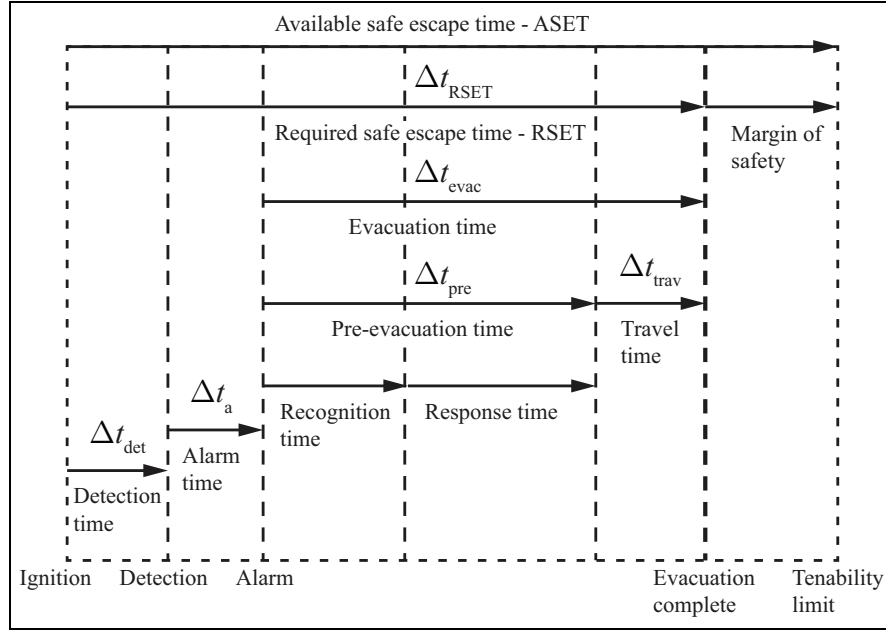


Figure 2. Simplified schematic of processes related to escape.⁴⁹

disturbing condition is estimated from the fire-related data on the visible part of the route, such as temperature and smoke concentration. If the condition is lethal, then the route will be excluded. Note that the exit selection algorithms are implemented with some approximation in the simulator.

3. Discussion about RSET/ASET calculations

In fire safety engineering terms it is necessary to ensure that ASET is greater than RSET by an appropriate margin of safety⁵⁰ (see Figure 2), that is:

$$\text{ASET} > \text{RSET} + \text{an appropriate safety margin}, \quad (11)$$

where ASET is the time from ignition to that when conditions become untenable to occupants, while RSET is the time from ignition to that when affected occupants are able to reach a place of safety.

3.1. RSET calculations

The basic formula determining RSET is shown as⁴⁹:

$$\text{RSET} = \Delta t_{det} + \Delta t_a + (\Delta t_{pre} + \Delta t_{trav}), \quad (12)$$

where Δt_{det} is the detection time, counted from ignition to detection by an automatic system or first occupant to detect fire cues. Δt_a is the alarm time, calculated from detection to a general alarm. Δt_{pre} is the pre-escape time, which includes two phases for each individual occupant, namely the recognition time Δt_{rec} and the response time Δt_{resp} . Δt_{trav} is the travel time, required for evacuees

to walk to a safe place. The evacuation time Δt_{evac} is the sum of the pre-movement time Δt_{pre} and the travel time Δt_{trav} . The available margin of safety can be determined by the difference between ASET and RSET.

3.2. ASET calculations

ASET may be generally calculated as:

$$\text{ASET} = \min\{T_{\text{smoke}}, T_{\text{heat}}, T_{\text{intoxication}}\}, \quad (13)$$

where T_{smoke} is the time from ignition to that when tenability limit of visibility is reached, T_{heat} is the time from ignition to that when tenability limit for exposure to radiant heat or convected heat is reached, $T_{\text{intoxication}}$ is the time from ignition to the moment that tenability of toxic gases is reached. Several reasonable tenability limits are established below.

3.2.1. Tenability criteria for the smoke. It is widely accepted that a design tenability limit of 5 m visibility should be used for small or domestic enclosures and 10 m visibility ($D \cdot m^{-1} = 0.08$) in large enclosures.³⁵ Nevertheless, it is assumed that passengers can easily locate evacuation routes and have the ability to evacuate through smoke in spite of the poor visibility, because of the simple layout of the platform (see Figure 3). Hence, the tenability criterion for smoke is not used to determine ASET.

3.2.2. Tenability criteria for exposure to fire and heat. In the simulation, the ventilation system will be activated to exhaust the effluent. According to Ji,⁵¹ when the

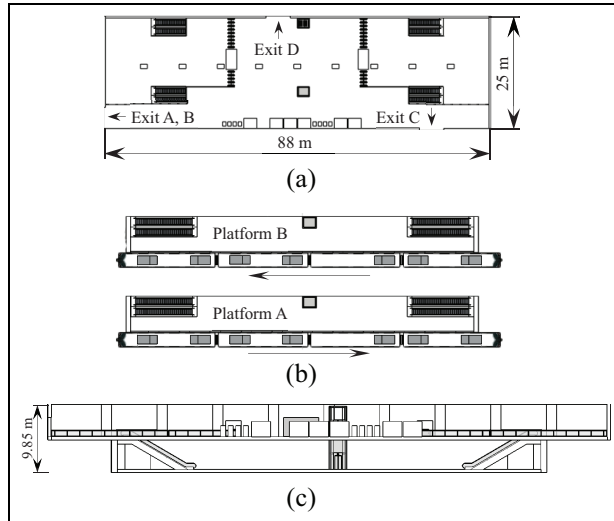


Figure 3. Layout of the station. (a) The station hall floor; (b) The platform floor; (c) Front view of the station.

mechanical exhaust system is activated for the smoke control in case of fire, the upper smoke layer no longer remains stable and would be mixed down to near floor level. In this case, passengers evacuate through dense smoke, exposed to radiant and convected heat simultaneously. Proposed tenability limits are 2.5 kW/m^2 for exposure to radiant heat, and 120°C for up to 7 minutes exposure to convected heat (water content of atmosphere $< 10\% \text{ H}_2\text{O}$ by volume).

3.2.3. Tenability criteria for toxic gases. Toxic gases in fires consist of a mixture of irritants and asphyxiants. Note that, a single fuel species composed primarily of C, H, O, and N is applied in the simulation, and hence irritants in the combustion products may be omitted. Asphyxiant gases, which are a main cause of incapacitation and death in fires, are carbon monoxide, hydrogen cyanide, carbon dioxide, and low oxygen. A predetermined total FED value, representing an acceptable incidence of incapacitation, may be set as the tenability limit of asphyxiant gases. Considering a considerable range of sensitivities to asphyxiants within the population, 0.3 FED is proposed for minimal effects on approximately 90% of the population.⁴⁹

In a word, the calculation of ASET in this paper may be simplified as:

$$\text{ASET} = \min\{T_{\text{heat}}, T_{0.3\text{FED}}\}, \quad (14)$$

where $T_{0.3\text{FED}}$ is the elapsed time from ignition to the moment that the total FED value is 0.3.

4. Simulation setting

4.1. Description of the metro station

First of all, a field measurement is conducted to obtain important information and parameters necessary for the

simulation, including the layout and size of the metro station, the ambient temperature and the wind speed, and temperature of vents. The measuring devices include a laser distance meter ($1.5 \text{ mm} \pm 5/100,000 \times \text{distance}$) and hot-wire anemometers ($\pm 0.5^\circ\text{C}$ for temperature and $\pm 0.1 \text{ m/s}$ for velocity). The measuring data are used for creating the 3D geometry model of the metro station and correcting the boundary condition of vents and exits.

The investigated side platform of the underground metro station in Guangzhou is called platform A. The whole station is 88 m long, 25 m wide, and 9.85 m high, as shown in Figure 3. The first underground floor of the station is the station hall floor with three exits to the outside, while the second is the platform floor, including two typical side platforms of the same layout. One elevator approximately in the middle and four escalators at both ends of the platform are used for two-way passenger transportation between the station hall and the platform.

The ventilation systems of the station are shown in Figure 4. There are two lines of air vents and one line of exhaust vents on the ceiling of the platform. Two lines of air vents are installed on the roof of the station hall. The operation mode settings of ventilation systems in normal conditions and fire cases are shown in Table 1. The ambient temperature of the station is set to be 26°C . These parameters are corrected and ultimately determined based on results from the field measurement. Table 2 shows that the temperature calculated by simulation agrees well with the measured value.

In case of fire, all the entrance/exit automatic fare gates in the station hall should be opened for efficient evacuation. It is assumed that no metro trains stop at the platform to avoid more casualties, and hence the PSDs are supposed to be shut tightly. Also, the elevator should not be used for evacuation.

According to China Code for Design of Metro,³³ the running speed of the escalator should be 0.65 m/s . As is known to all, the escalator may operate in three modes, namely the ascending mode, the descending mode, and the stop mode. The transition of the operation modes of escalators in the case of fire is studied to further understand its influence on the evacuation.

It is assumed that the detection time Δt_{det} is 10 s, 5 s after which a general alarm is activated, hence $\Delta t_a = 5 \text{ s}$. After the detection, the operation modes of all the devices related to fire evacuation, such as ventilation systems, automatic fare gates, will be changed into fire modes in 30 s.

4.2. Fire characteristics

The generic t^2 model is used to describe the growth phase and the fully developed phase of the fire. Fire on the platform may be easily caused by luggage and backpacks carried by passengers, filled with clothing, paper, books, etc. Hence, the fire is set with an ultrafast growth rate and a maximal HRR below 5 MW .⁵² The fire source is

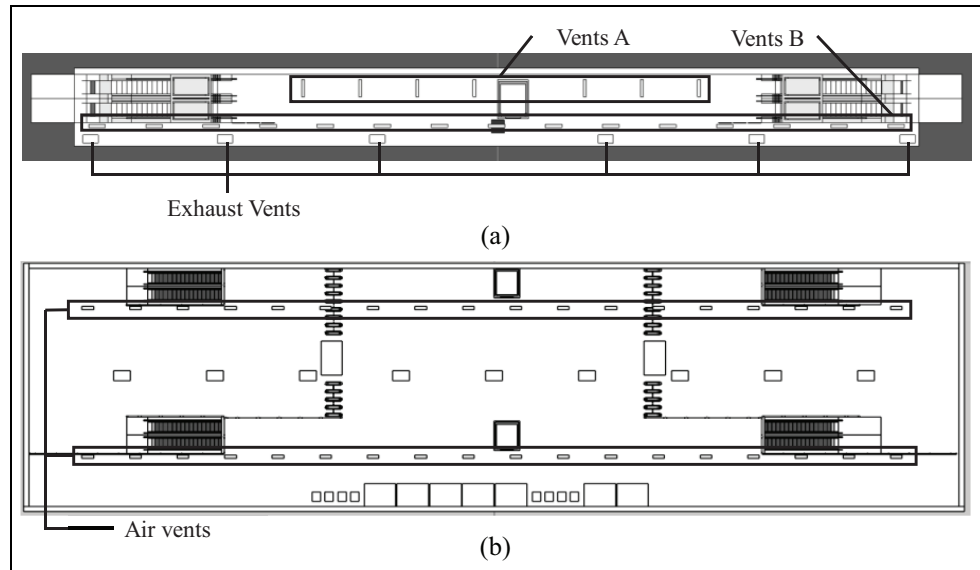


Figure 4. Ventilation systems. (a) Ventilation systems in the platform; (b) Ventilation systems in the hall.

Table 1. Operation mode settings of ventilation systems.

Case	Station hall	Platform A		Exhaust vents
	Air vents	Vents A	Vents B	
Normal	+ 0.8 m/s, 25 °C	+ 2 m/s, 24 °C	+ 0.8 m/s, 24 °C	/
Fire	+ 3.2 m/s, 25 °C	- 3.2 m/s	- 3.2 m/s	- 3.2 m/s

+ indicates air supplying mode, - indicates air exhausting mode, / indicates off mode.

Table 2. Temperature data validation (°C).

Position*	Measured	Simulation
Platform	24.3	24.3
Station hall	25.8	25.7
Exit A, B	25.9	25.8
Exit C	25.8	25.7
Exit D	25.3	25.3

*Data are obtained at the height of 1.5 m above the platform floor.

represented by a rectangle with a size of 1 m × 1 m. The fire growth curve is shown in Figure 5. Note that other flammable materials inside the platform are not considered.

Two parameters, the location and HRR of fire, may have a significant influence on the evacuation. Two fire locations are selected, namely the middle of the platform and the entrance of the escalators, as shown in Figure 6. Critical values of HRR are chosen as 1 MW, 2 MW, 3 MW and 5 MW.

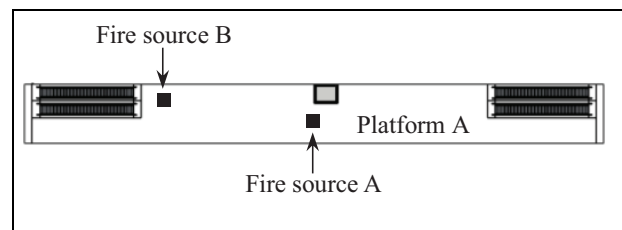


Figure 5. Location of fire sources.

4.3. Passenger characteristics

There are several default population types in the simulator, namely Adult, Male, Female, Child, and Elderly, which have different body dimensions and unimpeded walking speeds. Considering that the metro station is located at a university town in Guangzhou, most passengers are young university students, and the gender ratio is balanced in general. To reflect reality as accurately as possible, some modifications to the body dimensions and unimpeded walking speeds are applied to the default types, Male and Female. Critical values of the crowd density are selected as 1, 1.5,

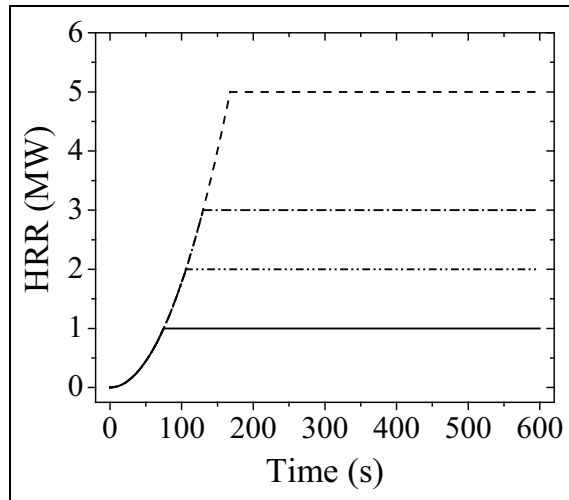


Figure 6. HRR curve.

2, and 2.5 person/m². All human parameters related to evacuation are listed in Table 3.

Concerning the pre-movement time Δt_{pre} , determined by passengers' recognition time and response time, it is assumed to obey a uniform distribution. The time interval is from 10 s to 30 s, considering the early detection by passengers close to the fire source and the message spread among passengers.

4.4. Fire scenarios

As shown in Table 4, 17 fire scenarios are developed for simulations, to study the influence on the fire evacuation of different factors (the fire location, HRR of fire, the operation mode of escalators, and the crowd density).

4.5. Simulation in parallel

To run the fire emergency evacuation simulator in parallel using MPI, the computational domain, containing the whole metro station, is divided into 128 meshes. After the mesh dependence analysis, 0.125 m is set as the cell size of the meshes in platform A, while the other meshes are

Table 3. Human parameters of different population types.

Population type	Gender ratio	Shoulder breadth (m)	Walking speed (m/s)			Δt_{pre} (s)
			Horizontal, unimpeded	On stationary escalators	On ascending escalators	
Male	0.5	0.500 ± 0.040	1.25 ± 0.20	0.6	1.2	[10, 30]
Female	0.5	0.435 ± 0.040	1.18 ± 0.20	0.6	1.2	[10, 30]

Table 4. Fire scenarios.

Scenario	Fire-human interaction	Fire source	HRR (MW)	Crowd density (person/m ²)	Operation mode	
					Ascending escalators	Descending escalators
S1	N	A	1	2	Up	Down
S2	Y	A	1	2	Up	Down
S3	Y	A	2	2	Up	Down
S4	Y	A	3	2	Up	Down
S5	Y	A	5	2	Up	Down
S6	Y	B	1	2	Up	Down
S7	Y	A	1	2.5	Up	Down
S8	Y	A	1	1.5	Up	Down
S9	Y	A	1	1	Up	Down
S10	Y	A	1	2	Up	Stop at $t_a + 30$ s
S11	Y	A	1	2	Up	Stop at $t_a + 40$ s
S12	Y	A	1	2	Up	Stop at $t_a + 50$ s
S13	Y	A	1	2	Up	Stop at $t_a + 60$ s
S14	Y	A	1	2	Up	Reverse at $t_a + 30$ s
S15	Y	A	1	2	Up	Reverse at $t_a + 40$ s
S16	Y	A	1	2	Up	Reverse at $t_a + 50$ s
S17	Y	A	1	2	Up	Reverse at $t_a + 60$ s

t_a indicates the moment of a general alarm.

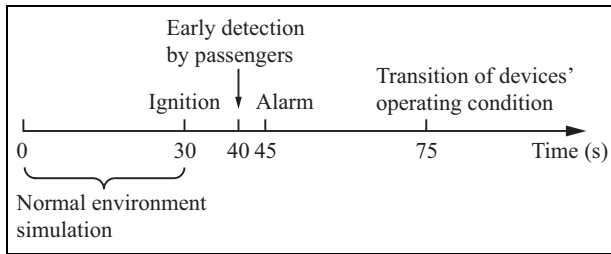


Figure 7. Timeline of the simulation.

relatively coarse. Mesh sensitivity studies suggest that these meshes are adequate, and the total grid number is around 2 million.⁶ The numerical simulation is realized on a 22-node Linux cluster, each node of which has two quad-core processors.

5. Simulation results

The timeline of the simulation is shown in Figure 7. The simulation results are summarized in Table 5. For each scenario, the simulation is run at least five times to obtain reliable results. The variations of the two listed quantities, maximal FED and RSET, are less than 10% and 3%, respectively. The results are considered to be sufficiently reliable for practical application.

5.1. Interaction between fire and humans

Unlike the fire drill, where evacuees are not affected by the fire and smoke, the evacuation in the case of fire may

be seriously influenced by dense smoke, heat, and toxic gases. For a better understanding of the interaction between fire and human behavior, a series of animated planar slices of the visibility, the air temperature, and the radiant heat flux of hot air are obtained at the height of 1.5 m above the platform floor. It is worth noting that the slices of the radiant heat flux are obtained by specifying several linear arrays of heat flux gauges in the simulator. The distance between each gauge is 0.5 m. The calculations of ASET are mainly based on these slices.

Take scenario S2 as an example. As illustrated in Figure 8, after ignition of the fire, the visibility inside the platform sharply declines below the tenability limit, 10 m, especially in the left portion of the platform. The dense smoke not only blocks the escape routes, but also slightly slows down the evacuation speed of passengers, which may increase the time for evacuation. Because of the limited exits, all passengers have no choice but to walk through the smoke and escape using the ascending escalators. Fortunately, according to the calculation of FED, the maximal FED is far below the tenability limit, 0.3, that is, nobody suffers from unconsciousness or even incapacitation caused by toxic gases. Figure 9 and Figure 10 indicate that neither the temperature nor the radiant heat flux of the air exceed the tenability limits in most regions of the platform, except close to the fire source.

Through the comparison between scenarios S1 and S2–S6, it is evident that the existence of fire affects the evacuation and increases RSET to various degrees, depending on the location and the HRR of the fire. Hence, the inter-

Table 5. Simulation results.

Scenario	Number of passengers in the platform A	Maximal FED ($\times 10^{-3}$)	RSET (s)	ASET (s)	Fire safety assessment
S1	480	0.000	136.6 \pm 1.6	/	/
S2	480	1.186 \pm 0.080	138.2 \pm 2.7	> 360	Safe
S3	480	1.937 \pm 0.167	143.5 \pm 3.6	> 360	Safe
S4	480	2.156 \pm 0.150	144.0 \pm 1.7	> 360	Safe
S5	480	2.576 \pm 0.226	146.2 \pm 2.1	> 360	Safe
S6	480	1.153 \pm 0.078	236.3 \pm 2.8	> 360	Safe
S7	594	2.005 \pm 0.043	167.9 \pm 2.3	> 360	Safe
S8	356	0.579 \pm 0.042	110.9 \pm 1.8	> 360	Safe
S9	238	0.151 \pm 0.020	84.3 \pm 2.2	> 360	Safe
S10	480	1.015 \pm 0.112	132.0 \pm 3.1	> 360	Safe
S11	480	0.995 \pm 0.073	137.0 \pm 3.0	> 360	Safe
S12	480	1.115 \pm 0.107	142.1 \pm 1.7	> 360	Safe
S13	480	1.190 \pm 0.078	144.0 \pm 2.5	> 360	Safe
S14	480	0.973 \pm 0.034	134.5 \pm 2.8	> 360	Safe
S15	480	0.978 \pm 0.077	138.5 \pm 2.5	> 360	Safe
S16	480	1.054 \pm 0.043	139.3 \pm 3.7	> 360	Safe
S17	480	1.031 \pm 0.061	139.4 \pm 1.3	> 360	Safe

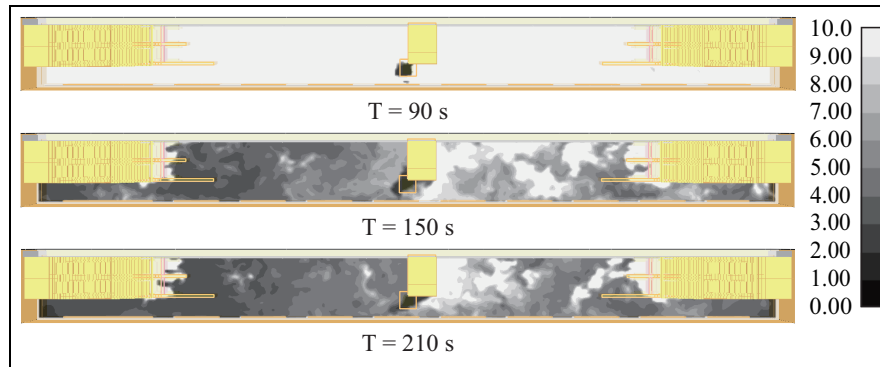


Figure 8. Visibility distribution (m).

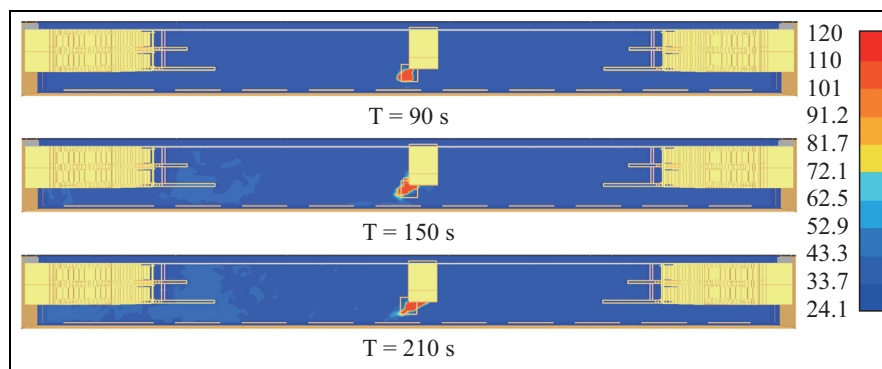


Figure 9. Temperature distribution ($^{\circ}\text{C}$).

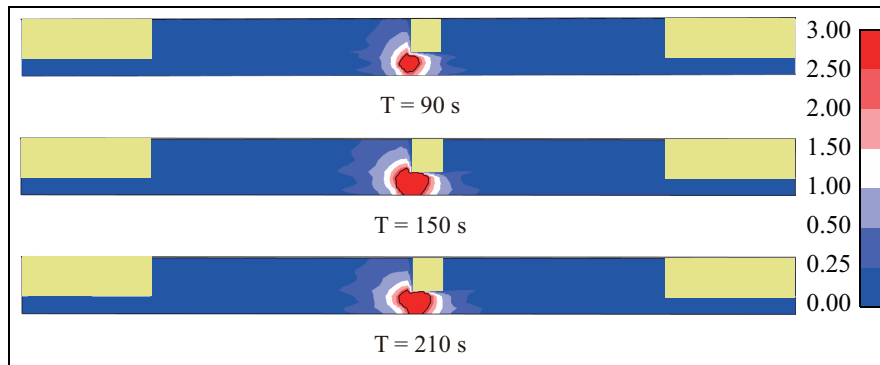


Figure 10. Radiant heat field (kW/m^2).

action between fire and human should not be neglected in the study of evacuation in the metro station.

5.2. Fire location

Two fire locations are selected for scenarios S2 and S6: one is in the middle of the platform, and the other is at the entrance of an escalator. As illustrated in Figure 11, RSET of scenario S6 is 58.3% longer than that of scenario S2. In

scenario S6, the left escalators are blocked by the fire and dense smoke, so that all passengers are forced to evacuate only through the right escalators. Hence, the fire location has a strong effect on the evacuation.

5.3. HRR of fire

On the one hand, as illustrated in Figure 12, there are minor differences on RSET between scenarios S1–S5. A

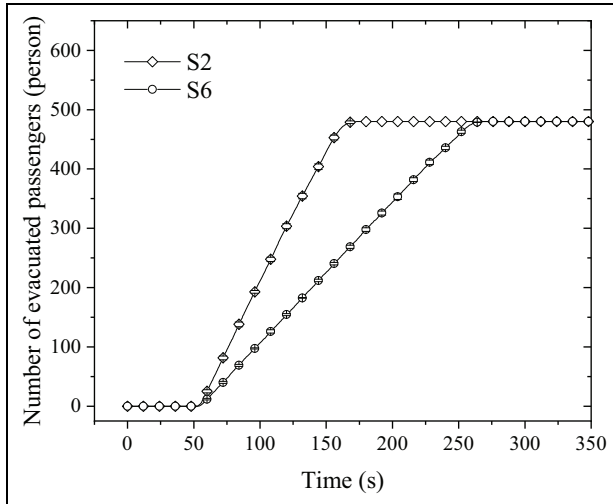


Figure 11. Relationship between the number of evacuated passengers and different fire locations.

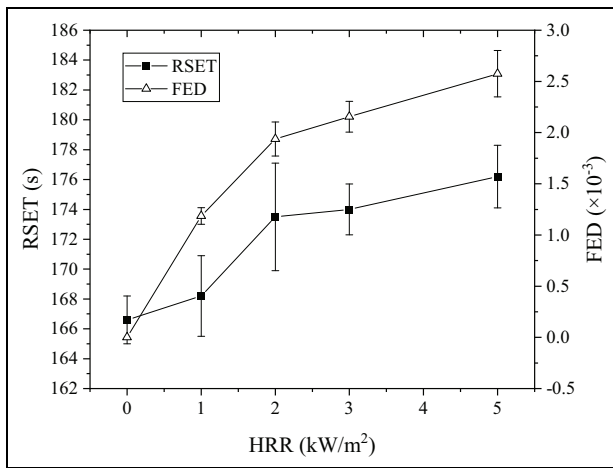


Figure 12. Effects of HRR on RSET and FED.

higher HRR of fire slightly increases RSET, which may be neglected in practice, however. On the other hand, the maximal FED grows with the increase of HRR of fire. Though the tenability limit of FED has not been reached, the simple combustion reaction used in this study means that the risk of intoxication should be noted. Therefore, HRR of the fire has a minor effect on the evacuation time, but closely relates to the intoxication of passengers.

5.4. Crowd density

The crowd density has a significant effect on the evacuation. In Figure 13, which shows the effects of crowd density on RSET and FED, RSET grows with the increase of the crowd density linearly. Meanwhile, as evacuation time extends, passengers stay longer on the platform filled with

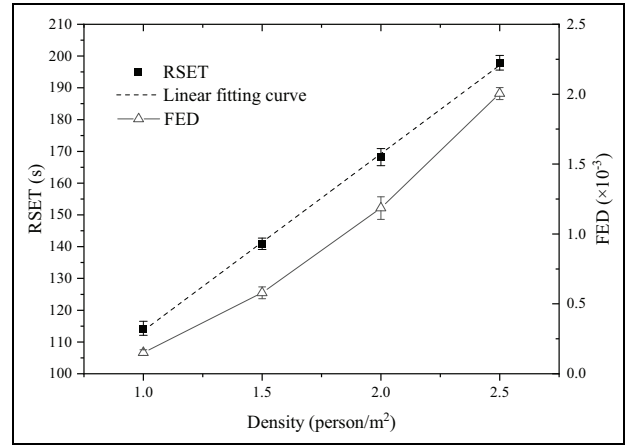


Figure 13. Effects of the crowd density on RSET and FED.

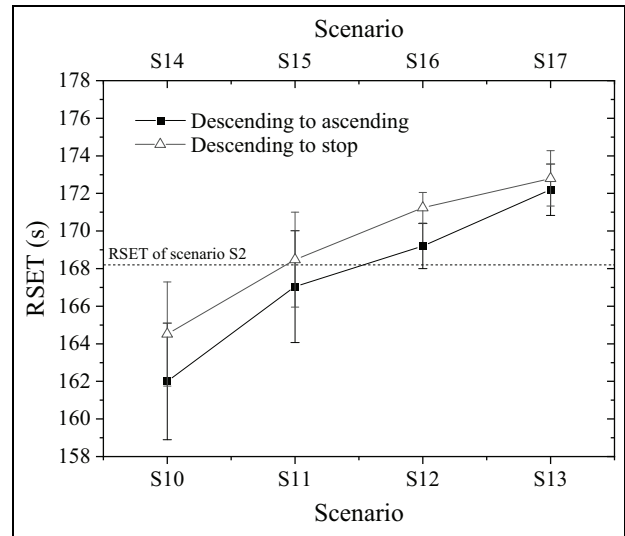


Figure 14. Relationship between RSET and transitions of the operation mode of descending escalators.

the dense smoke, causing the increase of FED. Hence, it is necessary to control the crowd density at an appropriate level for an efficient evacuation, in the case of fire. Moreover, RSET under different crowd densities is almost shorter than the corresponding ASET in scenarios S2, S7, S8, and S9, indicating that all passengers will be safely evacuated. As 2.5 person/m² is a relatively high crowd density, it can be concluded that the fire engineering design of the investigated platform enables safe evacuation for passengers.

5.5. The operation mode of escalators

Comparing scenarios S2, S10, and S14 in Figure 14, changing the descending escalators into ascending mode

has an effective impact on shortening the evacuation time and improving the evacuation efficiency, which performs better than stopping the descending escalators. RSET of S10 is 6.2 s shorter than that of S2, while the difference on RSET between S14 and S2 is only 3.7 s. In comparison with scenarios S10–S13, and S14–S17, only a change in the operation mode of descending escalators as early as possible can improve evacuation efficiency.

6. Conclusion

In this study, a fire evacuation coupled simulator is applied to investigate the fire evacuation process in a typical side platform of a metro station in Guangzhou. The ASET and RSET concept is applied in the safety assessment of fire evacuation, instead of the “6 minutes” principle widely used in China. A series of numerical simulations have been performed to investigate the influence of various factors such as the fire location, the HRR of fire, crowd density, and the operation mode of escalators on the fire evacuation. As the results show, the interaction between fire and human behavior should not be neglected in the evacuation simulation, as the existence of fire affects passengers’ behavior and increases the evacuation time to various degrees, depending on the fire location and the HRR of fire. The fire location is the main factor determining the distribution of smoke and heat, which strongly affects the evacuation route and passengers’ behavior. When the fire happens at the entrance of an escalator, RSET is 58.3% longer than that when the fire happens at the middle of the platform. Though having a minor effect on the evacuation time, the HRR is closely related to the intoxication of passengers. The crowd density is a crucial factor affecting the evacuation, for an increasing linear correspondence to RSET. It is vital to control the crowd density to an appropriate level for efficient evacuation. In addition, escalators have been used for evacuation in the metro station. Changing the escalators that normally operate in descending mode into the ascending mode can partly improve the evacuation efficiency. In the case of fire, metro station staff should change the existing operation mode of these descending escalators as early as possible.

The results will contribute to the design and the emergency management of similar types of metro stations to some extent. However, there are still some limitations to the present study. For instance, the simulation results have not been verified by experimental data obtained from a corresponding fire evacuation drill. Because of computing cost, only a lower limit is provided for the estimation of ASET. It would be better to conduct more extended simulations in the future to determine the exact value of ASET. Furthermore, extensive numerical simulations need to be conducted

for other types of the metro station of different layouts, to validate the influence of the factors mentioned in this paper. Moreover, other factors, such as the emergency operation mode of the ventilation system and the layout of escalators and staircases, also require further comprehensive research and analysis.

Funding

This research was funded by the national key R&D program for international collaboration and for HPC, grant number 2018YFE9103900 and 2016YFB0200603. The Natural Science Foundation of China (NSFC), grant number 11972384 and Guangdong MEPP Fund, grant number GDOE[2019] A01, and a grant from Guangzhou Science and Technology program, numbered 201704030089, also supported this work.

ORCID iD

Qinghe Yao  <https://orcid.org/0000-0003-1281-8603>

References

1. Ronchi E and Nilsson D. Basic concepts and modelling methods. In: Cuesta A, Abreu O and Alvear D editors. *Evacuation Modeling Trends*. Springer International Publishing, 2016, pp.1–23.
2. Hughes RL. A continuum theory for the flow of pedestrians. *Transport Res Part B Methodol* 2002; 36(6): 507–535.
3. Burstedde C, Klauck K, Schadschneider A, et al. Simulation of pedestrian dynamics using a two-dimensional cellular automaton. *Phys Stat Mech Appl* 2001; 295(3-4): 507–525.
4. Helbing D and Molnár P. Social force model for pedestrian dynamics. *Phys Rev E* 1995; 51(5): 4282–4286.
5. Marconi S and Chopard B. A multiparticle lattice gas automata model for a crowd. *Cellular Automata Proc* 2002; 2493: 231–238.
6. Chen K, Xie J and Yao Q. CFD simulation and analysis of smoke dispersion in a subway fire. *Acta Scient Natural Uni Sunyatseni* 2019; 58(2): 15–22.
7. Moriyama S, Hasemi Y, Nam DG, et al., editors. *Smoke movement characteristics and fire safety in subway stations*. International Association for Fire Safety Science, 2005.
8. Zhong W, Tu R, Yang JP, et al. A study of the fire smoke propagation in subway station under the effect of piston wind. *J Civ Eng Manag* 2015; 21(4): 514–523.
9. Gao R, Li A, Hao X, et al. Fire-induced smoke control via hybrid ventilation in a huge transit terminal subway station. *Energ Build* 2012; 45: 280–289.
10. Meng N, Hu L, Wu L, et al. Numerical study on the optimization of smoke ventilation mode at the conjunction area between tunnel track and platform in emergency of a train fire at subway station. *Tunnelling Underground Space Technol* 2014; 40: 151–159.
11. Rie DH, Hwang MW, Kim SJ, et al. A study of optimal vent mode for the smoke control of subway station fire. *Tunnelling Underground Space Technol* 2006; 21(3-4): 300–301.

12. Giachetti B, Couton D and Plourde F. Smoke spreading analyses in a subway fire scale model. *Tunnelling Underground Space Technol* 2017; 70: 233–239.
13. Zhou R, He J, Jiang J, et al. Smoke diffusion and control at different platform floor structure of subway station in fire. *Zhongguo Tiedao Kexue/China Railway Sci* 2008; 29(6): 126–131.
14. Roh JS, Ryou HS, Park WH, et al. CFD simulation and assessment of life safety in a subway train fire. *Tunnelling Underground Space Technol* 2009; 24(4): 447–453.
15. Roh JS, Ryou HS and Yoon SW. The effect of PSD on life safety in subway station fire. *J Mech Sci Technol* 2010; 24(4): 937–942.
16. Shi C, Zhong M, Nong X, et al. Modeling and safety strategy of passenger evacuation in a metro station in China. *Saf Sci* 2012; 50(5): 1319–1332.
17. Zhong MH, Shi CL, Tu XW, et al. Study of the human evacuation simulation of metro fire safety analysis in China. *J Loss Prevent Process Ind* 2008; 21(3): 287–298.
18. Tsukahara M, Koshiba Y and Ohtani H. Effectiveness of downward evacuation in a large-scale subway fire using Fire Dynamics Simulator. *Tunnelling Underground Space Technol* 2011; 26(4): 573–581.
19. Wan JH, Sui J and Yu H. Research on evacuation in the subway station in China based on the Combined Social Force Model. *Phys A Stat Mech Appl* 2014; 394: 33–46.
20. Frantzich H and Nilsson D. *Utrymning genom tät rök: beteende och förflyttning: Fire Safety Engineering and Systems Safety*, 2003.
21. Yang X, Dong H, Yao X, et al. Pedestrian evacuation at the subway station under fire. *Chin Phys B* 2016; 25(4): 48902–048902.
22. Yang P, Li C and Chen D. Fire emergency evacuation simulation based on integrated fire-evacuation model with discrete design method. *Adv Eng Software* 2013; 65: 101–111.
23. Tian J. *Study on Human Behavior in Metro Fire and Risk Analysis*. PhD thesis, Guangzhou University, Guangzhou, 2006.
24. Wang XD, Chen SK, Zhou YF, et al. Simulation on passenger evacuation under fire emergency in metro station. In: *2013 IEEE International Conference on Intelligent Rail Transportation (ICIRT)*. 2013, pp.260–263.
25. Han X, He X and Cong B. Simulation analysis of traffic capacity for ticket gates of metro station. In: *2011 International Conference on Electronic Engineering, Communication and Management, EECM 2011*. Beijing, 2012. pp.549–553.
26. Liao M, Liu G and Qiu TZ. Passenger traffic characteristics of service facilities in rail transit stations of Shanghai. *J Transport Eng* 2013; 139(2): 223–229.
27. Fujii K and Sano T. Experimental study on crowd flow passing through ticket gates in railway stations. *Transport Res Procedia* 2014; 630–635.
28. Liao W, Zheng X, Cheng L, et al. Layout effects of multi-exit ticket-inspectors on pedestrian evacuation. *Saf Sci* 2014; 70: 1–8.
29. Ding J, Zhang R, Yang J, et al. Research on the optimization of transport hub set up automatic fare machine based on simulation analysis. *Road Traffic Saf* 2016; 16(1): 43–49.
30. Okada N, Hasemi Y and Moriyama S. Feasibility of upward evacuation by escalator - An experimental study. *Fire Mater* 2012; 36(5–6): 429–440.
31. Kadokura H, Sekizawa A and Takahashi W. Study on availability and issues of evacuation using stopped escalators in a subway station. *Fire Mater* 2012; 36(5–6): 416–428.
32. Hou Z, Zhong M, Shi C, et al. Effect of escalator movement mode on passenger evacuation from subway station. *Fire Sci Technol* 2015; 34(4): 449–451.
33. Standard CN. GB 50157-2013. *Code for design of metro*. Beijing: China Architecture & Building Press, 2013.
34. Purser DA. Developments in tenability and escape time assessment for evacuation modelling simulations. In: Cuesta A, Abreu O and Alvear D (eds) *Evacuation Modeling Trends*. Cham: Springer International Publishing, 2016, pp.25–53.
35. Zhang B, Zhang J and Meng Y. Study on establishing personnel safety criteria in performance-based fire design. *Chin Saf Sci J* 2017; 27(2): 41–46.
36. Ma C, Sun B, Sun S, et al. Analysis of performance-based fire safety evacuation in a college library. *Procedia Eng* 2012; 43: 399–406.
37. Sujatmiko W, Dipojono HK, Soelami FXN, et al. Performance-based fire safety evacuation in high-rise building flats in Indonesia – A case study in Bandung. *Procedia Env Sci* 2014; 20: 116–125.
38. McGrattan K, Hostikka S, McDermott R, et al. *Fire Dynamics Simulator User's Guide*. Sixth edn. NIST Special Publication, 2017.
39. Deardorff JW. Stratocumulus-capped mixed layers derived from a 3-dimensional model. *Boundary-Layer Meteorol* 1980; 18(4): 495–527.
40. Pope SB. *Turbulent flows*. Cambridge: Cambridge University Press, 2000.
41. Sweet RA. Direct methods for the solution of Poisson's equation on a staggered grid. *J Comput Phys* 1973; 12(3): 422–428.
42. Helbing D, Farkas IJ, Molnar P, et al. *Simulation of pedestrian crowds in normal and evacuation situations*. In: Schreckenberg M and Sharma SD (eds) *Pedestrian and evacuation dynamics*. Duisburg, Germany: Springer, 2002, p. 58.
43. Korhonen T. *Fire dynamics simulator with evacuation: FDS + Evac technical reference and user's guide*. VTT Technical Research Center of Finland, 2017.
44. Purser DA and McAllister JL. Assessment of hazards to occupants from smoke, toxic gases, and heat. In: Hurley MJ, Gottuk D, Hall JR, et al. (eds) *SFPE handbook of fire protection engineering*. New York, NY: Springer New York, 2016, pp.2308–2428.
45. Purser D. Toxicity assessment of combustion products. *SFPE handbook of fire protection engineering*. Third edn. Quincy, Massachusetts: National Fire Protection Association, 2002, p. 2-83-82-171.
46. Korhonen T and Hostikka S. *Fire dynamics simulator with evacuation: FDS + Evac technical reference and user's guide*. Espoo, Finland: VTT Technical Research Centre of Finland, 2009.
47. Ehtamo H, Heliövaara S, Korhonen T, et al. Game theoretic best-response dynamics for evacuees' exit selection. *Adv Complex Syst* 2010; 13(1): 113–134.

48. Ehtamo H, Heliövaara S, Hostikka S, et al., editors. *Modeling evacuees' exit selection with best response dynamics*. Berlin, Heidelberg: Springer, 2010.
49. Institution BS. PD 7974-6:2004. *The application of fire safety engineering principles to fire safety design of buildings—Part 6: Human Factors: Life safety strategies—Occupant evacuation, behaviour and condition*. London: British Standards Institution, 2004.
50. Purser D. ASET and RSET: Addressing some issues in relation to occupant behaviour and tenability. *Fire Safety Science* 2003; 7: 91–102.
51. Ji J. *Studies on smoke movement and ventilation control mode in subway station fire*. PhD thesis, University of Science and Technology of China, 2008.
52. Yang Y and Cao L. Preparatory study on scenario design for subway fire. *J Nat Disasters* 2006; 15(4): 121–125.

Author biographies

Jiabin Xie is an undergraduate student majoring in the department of theoretical and applied mechanics at the Sun Yat-sen University.

Kecheng Chen is an undergraduate student majoring in the department of theoretical and applied mechanics at the Sun Yat-sen University.

Trevor Hocksun Kwan is a postdoctoral researcher in the department of theoretical and applied mechanics at the Sun Yat-sen University.

Qinghe Yao is an associate professor in the department of theoretical and applied mechanics at the Sun Yat-sen University.